J|A|C|S
ARTICLES
Published on Web 11/13/2002

Roles of the Proximal Hydrogen Bonding Network in Cytochrome $P450_{cam}$-Catalyzed Oxygenation

Shiro Yoshioka,[†,§] Takehiko Tosha,[†] Satoshi Takahashi,[†] Koichiro Ishimori,[†] Hiroshi Hori,[‡] and Isao Morishima*[,†]

Contribution from the Department of Molecular Engineering, Graduate School of Engineering, Kyoto University, Kyoto, 606-8501, Japan and Division of Biophysical Engineering, Graduate School of Engineering, Osaka University, Toyonaka, Osaka, 560-8531, Japan

Received April 16, 2002

Abstract: Structural and functional roles of the hydrogen bonding network that surrounds the heme-thiolate coordination of $P450_{cam}$ from *Pseudomonas putida* were investigated. A hydrogen bond between the side chain amide of Gln360 and the carbonyl oxygen of the axial Cys357 was removed in Q360L. The side chain hydrogen bond and the electrostatic interaction between the polypeptide amide proton of Gln360 and the sulfur atom of Cys357 were simultaneously removed in Q360P. The increased electron donation of the axial thiolate in Q360L and Q360P was evidenced by negative shifts of their reduction potentials by 45 and 70 mV, respectively. Together with the results on L358P in which the amide proton at position 358 was removed (Yoshioka, S., Takahashi, S., Ishimori, K., Morishima, I. *J. Inorg. Biochem.* **2000**, *81*, 141−151), we propose that the side chain hydrogen bond and the electrostatic interaction of the amide proton with the thiolate ligand cause ∼45 and ∼35 mV of positive shifts, respectively, of the redox potential of the heme in $P450_{cam}$. The resonance Raman spectra of the ferrous-CO form of the Q360 mutants showed a downshifted Fe−CO stretching mode at 482∼483 cm^{-1} compared with that of wild-type $P450_{cam}$ at 484 cm^{-1}. The Q360 mutants also showed the upshift by 4∼5 cm^{-1} of the Fe−NO stretching mode in the ferrous-NO form. These Raman results indicate the increase in the σ-electron donation of the thiolate ligand in the reduced state of the Q360 mutants and were in contrast to the increased π-back-donation of the thiolate in L358P having an upshifted Fe−CO stretching mode at 489 cm^{-1}. The catalytic activities of the Q360 mutants for the unnatural substrates were similar to those of the wild-type enzyme, indicating that the increased σ-electron donation does not promote the O−O bond heterolysis in the Q360 mutants, although the increased π-electron donation in L358P promoted the heterolysis of the O−O bond. We conclude that the functions of the proximal hydrogen bonding network in $P450_{cam}$ are to stabilize the heme-thiolate coordination, and to regulate the redox potential of the heme iron. Furthermore, we propose that the π-electron donation, not the σ-electron donation, of the thiolate ligand promotes the heterolysis of the O−O bond of dioxygen.

Introduction

Heme-containing enzymes such as cytochrome P450 (P450), chloroperoxidase (CPO), and nitric oxide synthase (NOS) activate dioxygen or hydrogen peroxide using the heme iron and catalyze insertions of the activated oxygen atom into various substrates of physiological importance.[1] The common structural characteristic of these enzymes is the heme-thiolate (Fe−S^-) coordination in their active sites.[2] The strong electron-releasing character of the thiolate ligand has been assumed to serve as the "push" effect that enables the heterolytic O−O bond scission to generate the activated iron (IV)-oxo species commonly called compound I.[3] Furthermore, the electronegative thiolate group should determine the redox potential of the heme in these enzymes to accept electrons from their redox partners and to stabilize the electron-deficient active species.[4] However, the regulation mechanism of these functions by the thiolate ligand has not been fully clarified.

Recently, the conserved NH−S hydrogen bonds between the thiolate ligand and the protons from the surrounding polypeptide amides have been assumed to control the functions of the heme-thiolate enzymes by neutralizing the negative charge on the thiolate.[5] For example, the sulfur atom of the axial thiolate (Cys357) in $P450_{cam}$ from *Pseudomonas putida* is surrounded by three amide protons of Leu358, Gly359, and Gln360[6] with

* To whom correspondence should be addressed. Tel: +81-75-753-5945. Fax: +81-75-751-7611. E-mail: morisima@mds.moleng.kyoto-u.ac.jp.
† Department of Molecular Engineering, Graduate School of Engineering, Kyoto University.
‡ Division of Biophysical Engineering, Graduate School of Engineering, Osaka University.
§ Current address: Department of Biochemistry, Vanderbilt University, Nashville, TN 37232-0146.

(1) Ortiz de Montellano, P. R., Ed. *Cytochrome P450 Structure, Mechanism and Biochemistry*; Plenum: New York, 1995.
(2) Mansuy, D.; Renaud, J.-P. In *Cytochrome P450 Structure, Mechanism and Biochemistry*, 2nd ed.; Ortiz de Montellano, P. R., Ed.; Plenum: New York, 1995; pp 537−574.
(3) Sono, M.; Roach, M. P.; Coulter, E. D.; Dawson, J. H. *Chem. Rev.* **1996**, *96*, 2841−2887.
(4) Poulos, T. L.; Cupp-Vickery, J.; Li, H. In *Cytochrome P450 Structure, Mechanism, and Biochemistry*, 2nd ed; Ortiz de Montellano, P. R., Ed.; Plenum Press: New York, 1995 pp 125−150.
(5) Poulos, T. L. *J. Biol. Inorg. Chem.* **1996**, *1*, 356−359.

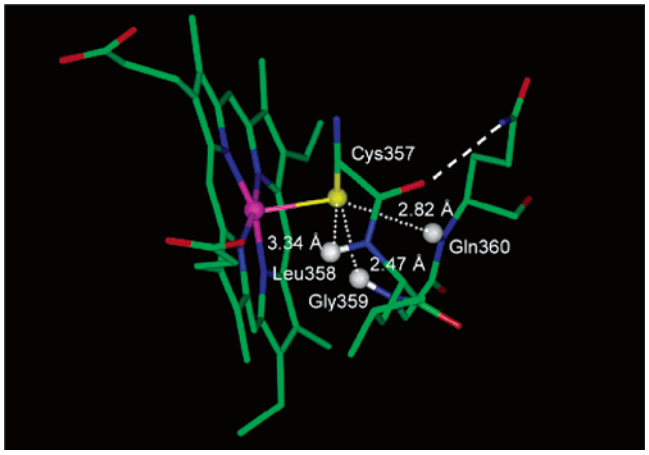

Figure 1. Proximal hydrogen bonding network of cytochrome $P450_{cam}$. The purple, yellow, and white balls indicate the heme iron, the sulfur atom of Cys357, and the main chain amide protons at Leu359, Gly359, and Gln360, respectively. The dotted lines indicate the NH−S hydrogen bonds that surround the axial thiolate ligand. The broken line indicates the hydrogen bond between the side chain amide of Gln360 and the main chain carbonyl of Cys357. The amide protons were generated by Discover (SGI) based on the X-ray coordinates (2cpp)(6). This figure was created by Insight II (SGI).

the estimated H−S distances of 3.34, 2.47, and 2.82 Å, respectively (Figure 1). Although the NH−S units for Leu358 and Gln360 deviate significantly from the linear conformation, the partial positive charges of these protons should give electrostatic interactions with the thiolate sulfur.[4,5] These NH−S hydrogen bonds are also found in other P450 enzymes such as $P450_{eryF}$, $P450_{BM-3}$, and $P450_{terp}$.[7−9] CPO utilizes two of the three NH−S hydrogen bonds, in which one hydrogen bond is lost by the introduction of a proline residue.[10] The thiolate ligand in NOS accepts an additional hydrogen bond from the indole NH of Trp, thus allows the formation of one more NH−S hydrogen bond than that found in CPO.[11] Poulos pointed out that the NH−S hydrogen bonds might stabilize the coordination of the anionic thiolate ligand to the reduced heme iron, and also control the redox potential of the heme and the push effect of the thiolate ligand.[4,5]

The proposed roles of the NH−S hydrogen bonds were partially confirmed using heme-thiolate model complexes. The arene-thiolate compounds prepared by Ueyama et al. revealed that the hydrogen bonds between amide protons and sulfur atom increase the redox potential of the heme and stabilize the coordination of the sulfur atom.[12,13] The alkane-thiolate compound prepared by Suzuki et al. also indicated that the NH−S hydrogen bond increases the heme redox potential and stabilizes the heme-sulfur coordination. Furthermore, it was observed that the NH−S hydrogen bond affects the monooxygenation activity for hydrocarbons.[14] The recent study by Ueno et al. using the tetrapeptide-heme complexes that mimicked the proximal strructure of $P450_{cam}$ also demonstrated the increase of the redox potential by the NH−S hydrogen bonding.[15]

The roles of the NH−S hydrogen bonds were recently extended in the theoretical consideration of the activated species of P450 reaction.[16,17] The electronic structures of the putative compound I in P450 were calculated using the density functional theory (DFT) by Shaik et al., indicating that the NH−S hydrogen bonds and the polarity around the heme localized the unpaired electron spin to an a_{2u} orbital of porphyrin ring. On the contrary, the absence of the NH−S hydrogen bonds localizes the unpaired electron at the sulfur atom. The NH−S hydrogen bonds might therefore be important in controlling the reactivity of compound I in P450.

In contrast to the model complex and theoretical investigations, the verifications of the proposed roles of the NH−S hydrogen bonds in actual P450 enzymes have been limited. The importance of the hydrogen bonds for the stability of the heme-thiolate coordination was at least evident, because attempts to substitute the axial cysteine with histidine in $P450_{cam}$ by us[18] and by others[19] suffered serious structural alterations around the heme, which are likely caused by the disruption of the NH−S hydrogen bonding.[18] Furthermore, the single substitutions of axial histidine with cysteine in myoglobin and in cytochrome *c* peroxidase do not form stable heme-thiolate coordination upon the reduction of heme iron.[20,21]

To understand the electronic effects of the NH−S hydrogen bonds on the redox potential and the activities in $P450_{cam}$, we removed one of the amide protons in order to modulate the negative charge on the sulfur atom.[22] To accomplish this, we introduced a proline residue at position 358, which is adjacent to the proximal cysteine (L358P of $P450_{cam}$). We found that the reduction potential of the heme iron in L358P showed a negative shift by 35 mV, which implies the increase in the electronic push effect by the deletion of one of the amide protons. Resonance Raman experiments for the ferrous-carbonmonoxy form of L358P revealed the increase of π-back-donation from thiolate to iron. Furthermore, the increased electron density of the thiolate in L358P depressed the uncoupling reaction (formation of hydrogen peroxide), when the unnatural substrates such as styrene and cyclohexane were used instead of the natural substrate, *d*-camphor. These results clearly indicated that the electron density on the thiolate, which is modulated by the removal of the amide proton at position 358, is one of the determinants for the redox potential of the heme and the O−O bond heterolysis in $P450_{cam}$.[22]

(6) Poulos, T. L.; Finzel, B. C.; Howard, A. J. *J. Mol. Biol.* **1987**, *195*, 687−700.
(7) Cupp-Vickery, J.; Poulos, T. L. *Nat. Struct. Biol.* **1995**, *2*, 144−153.
(8) Ravichandran, K. G.; Boddupalli, S. S.; Hasemann, C. A.; Peterson, J. A.; Deisenhofer, J. *Science* **1993**, *261*, 731−736.
(9) Hasemann, C. A.; Ravichandran, K. G.; Boddupalli, S. S.; Perterson, J. A.; Deisenhofer, J. *Structure* **1995**, *3*, 41−62.
(10) Sundaramoorthy, M.; Terner, J.; Poulos, T. L. *Structure* **1995**, *3*, 1367−1377.
(11) Crane, B. R.; Arvai, A. S.; Gachhui, R.; Wu, C.; Ghosh, D. K.; Getzoff, E. D.; Stuehr, D. J.; Tainer, J. A. *Science* **1997**, *278*, 425−431.
(12) Ueyama, N.; Nishikawa, N.; Yamada, Y.; Okamura, T.; Nakamura, A. *J. Am. Chem. Soc.* **1996**, *118*, 12 826−12 827.
(13) Ueyama, N.; Nishikawa, N.; Yamada, Y.; Okamura, T.; Oka, S.; Sakurai, H.; Nakamura, A. *Inorg. Chem.* **1998**, *37*, 2415−2421.
(14) Suzuki, N.; Higuchi, T.; Urano, Y.; Kikuchi, K.; Uekusa, H.; Ohashi, Y.; Uchida, T.; Kitagawa, T.; Nagano, T. *J. Am. Chem. Soc.* **1999**, *121*, 11 571−11 572.
(15) Ueno, T.; Nishikawa, N.; Moriyama, S.; Adachi, S.; Lee, K.; Okamura, T.; Ueyama, N.; Nakamura, A. *Inorg. Chem.* **1999**, *38*, 1199−1210.
(16) Schöneboom, J. C.; Lin, H.; Reuter, N.; Thiel, W.; Cohen, S.; Ogliaro, F.; Shaik, S. *J. Am. Chem. Soc.* **2002**, *124*, 8142−8151.
(17) de Visser, S. P.; Ogliaro, F.; Sharma, P. K.; Shaik, S. *Angew. Chem., Int. Ed.* **2002**, *41*, 1947−1951.
(18) Yoshioka, S.; Takahashi, S.; Hori, H.; Ishimori, K.; Morishima, I. *Eur. J. Biochem.* **2001**, *268*, 252−259.
(19) Auclair, K.; Moënne-Loccoz, P.; Ortiz de Montellano, P. R. *J. Am. Chem. Soc.* **2001**, *123*, 4877−4885.
(20) Adachi, S.; Nagano, S.; Ishimori, K.; Watanabe, Y.; Morishima, I.; Egawa, T.; Kitagawa, T.; Makino, R. *Biochemistry* **1993**, *32*, 241−252.
(21) Sigman, J. A.; Pond, A. E.; Dawson, J. H.; Lu, Y. *Biochemistry* **1999**, *38*, 11 122−11 129.
(22) Yoshioka, S.; Takahashi, S.; Ishimori, K.; Morishima, I. *J. Inorg. Biochem.* **2000**, *81*, 141−151.

In this study, we focus our attention on the proximal hydrogen bonding network including the conserved NH−S hydrogen bonds in P450$_{cam}$ for further clarification on the roles of the proximal structure. We noticed that the amide protons at positions 358 and 360 approach the sulfur atom of Cys357 from different directions, which may modulate different electronic effects on the thiolate ligand (Figure 1). Furthermore, the side chain amide of Gln360 forms a second hydrogen bond with the carbonyl oxygen of Cys357 (Figure 1),[15,16] which could play an electronic or structural role in the heme-thiolate coordination. Thus, we choose the glutamine residue at position 360 as the target for the current mutational study. It is expected that the mutation of Gln360 with leucine (Q360L) removes only the side chain hydrogen bond, and that the mutation with proline (Q360P) removes both of the NH−S hydrogen bond and the side chain hydrogen bond. We intend to dissect the contributions of the different interactions to the structural and functional properties of P450$_{cam}$ by comparing the properties of Q360L, Q360P, and L358P.

We constructed the Q360P and Q360L mutants of P450$_{cam}$ and characterized their structural and electronic changes using spectroscopic methods such as resonance Raman, EPR, and NMR. Comparing the data of the Q360 mutants with those for wild type and L358P, we discuss the electronic effects of the thiolate ligand and roles of the proximal hydrogen bonding network on the P450$_{cam}$ functions.

Materials and Methods

Materials. *E. coli* strains used in this study were the same as those described previously.[18,22] Mutagenesis was performed on M13mp19 using Kunkel method.[23] The expression vector of P450$_{cam}$ was pT7-P450$_{cam}$.[18,22] The plasmids were prepared by the rapid alkaline extraction method and purified by the standard method.[24] Oligonucleotides were purchased from Rikaken (Nagoya, Japan) or Invitrogen Japan (Tokyo, Japan). Restriction enzymes, T4 polynucleotide kinase and T4 DNA ligase, were purchased from Takara (Kyoto, Japan). A ligation kit from Takara was used for the plasmid preparations. DNA sequencing was carried out using a DNA sequencer (Perkin-Elmer, Model 373A). General organic and inorganic compounds were purchased from Wako (Osaka, Japan) or Nakalai Tesque (Kyoto, Japan) as the highest quality available, and used without further purification.

Expression and Purification of P450$_{cam}$ and Other Proteins. The wild type, L358P and Q360 mutants were expressed and purified according to the method described previously.[18,22] Putidaredoxin (Pdx) and putidaredoxin reductase (PdR) were prepared according to the reported method.[25] The purified Pdx had the 325 to 280 nm absorbance ratio of at least 0.6. The purified PdR had the 325 to 280 nm absorbance ratio of 0.68.

Spectroscopic Measurements. Electronic absorption spectra were recorded on a Lambda-18 spectrophotometer (Perkin-Elmer) at room temperature. The ferrous proteins were prepared by adding a small amount of sodium dithionite anaerobically, and the CO-bound proteins were obtained by the dithionite reduction after CO bubbling. The sample solutions contained 10 μM of proteins, 50 mM of potassium phosphate at pH 7.4, 100 mM of KCl, and 1 mM of *d*-camphor.

Electron paramagnetic resonance (EPR) spectra were obtained at X-band (9.22 GHz) microwave frequency using a Varian E−12 spectrometer with 100-kHz field modulation. An Oxford helium cryostat (ESR-900) was used for measurements at 15 K. The sample concentration was 60 μM dissolved in the same buffer used for the optical absorption measurements.

The Fe−S stretching lines of the resonance Raman spectra for the ferric proteins were obtained by a laser excitation at 363.8 nm from an Ar ion laser (Spectra Physics, Beamlok 2080). Resonance Raman data for the ferric and ferrous proteins were obtained by exciting at 413.1 nm from a Kr ion laser (Spectra Physics, Model 2016). Resonance Raman data for the CO- and NO-bound proteins were obtained by exciting at 441.6 nm from a He−Cd laser (Kinmon Electronics, CCDR80SG). The detection was performed by a single polychromator (Ritsu, DG-1000) equipped with a liquid nitrogen-cooled CCD camera (Astromed, CCD3200 or Princeton Instruments, CCD-1100PB). The frequencies of the Raman lines were calibrated with indene. Spinning quartz cells were used to avoid a protein denaturation by the laser irradiation. All measurements were performed at room temperature. The sample concentrations were 100 and 15 μM for the spectra measured using UV and visible laser excitations, respectively. All samples were dissolved in the same buffer used for the optical absorption measurements.

Proton nuclear magnetic resonance (^{1}H NMR) spectra for the cyanide-bound proteins were measured on a Bruker Avance DRX500 spectrometer at 290 K. Chemical shifts were referenced to tetramethylsilane (TMS). We employed the WET pulse sequence to minimize the water signal.[26] The sample solutions contained 400 μM of proteins, 50 mM of potassium phosphate at pH 7.4, 1 mM of *d*-camphor, 10% of D_2O, and 10 mM of KCN.

Reduction Potential Measurements. The midpoint potentials (E_0) of P450$_{cam}$ were obtained from the plots of the monitored electrode potential (E_h) against the percentage of the reduced P450$_{cam}$ at 25 °C. The plots were fitted with the Nernst equation.[27] Safranine T, phenosafranine, benzyl viologen, and α-hydroxyphenazine were added as mediators to the sample solutions containing 50-mM potassium phosphate at pH 7.0, 50-mM EDTA, and ca. 10-μM P450$_{cam}$. The midpoint potentials were calibrated by utilizing phenosafranine (−252 mV) as a standard.[28] All potentials were recalculated with the reference to NHE.

P450$_{cam}$ Activity Measurements. Catalytic activities of P450$_{cam}$ for *d*-camphor and hydrocarbons were measured by monitoring the consumption rates of NADH at 25 °C. The standard assay mixture contained 0.5-μM P450$_{cam}$, 0.5-μM PdR, 5-μM Pdx, 200-μM NADH, and 1-mM *d*-camphor or 1.7∼2.0 mM of the unnatural substrates in 50-mM potassium phosphate at pH 7.4. For the Michaelis−Menten analysis, the concentration of Pdx was changed from 5 to 20 μM. The reactions were initiated by the addition of the P450$_{cam}$ to the final concentration of 0.5-μM and monitored at the 340-nm absorption band of NADH. The NADH consumption rates were calculated using an extinction coefficient of 6.22 mM^{-1} cm^{-1} for NADH. The observed changes were linear against the elapsed time for *d*-camphor and cyclohexane, but not linear for styrene. The products were confirmed by gas chromatography on Shimadzu GC-18A equipped with a flame-ionization detector and a DB-1701 column (J & W Scientific). Benzyl alcohol and chlorobenzene were used as the internal standards. Experimental errors of the product quantitations were less than 7%.

The H_2O_2 productions in the reactions with *d*-camphor and unnatural substrates were quantitated using the iron thiocyanate colorimetric assay as described by Atkins et al.[29,30] A 500-μL portion of 10-mM ferrous ammonium sulfate and 100 μL of 0.5-M potassium thiocyanate were

(23) Kunkel, T. A.; Roberts, J. D.; Zakour, R. A. *Methods Enzymol.* **1987**, *154*, 367−382.
(24) Sambrook, J.; Fritsch, E. F.; Maniatis, T. *Molecular Cloning. A Laboretory Manual*; Cold Spring Harbor Laboratory Press: Cold Spring Harbor, New York, 1989.
(25) Aoki, M.; Ishimori, K.; Morishima, I. *Biochim. Biophys. Acta* **1998**, *1386*, 157−167.
(26) Ogg, R. J.; Kingsley, P. B.; Taylor, J. S. *J. Magn. Res., Ser. B* **1994**, *104*, 1−10.
(27) Yamada, H.; Makino, R.; Yamazaki, I. *Arch. Biochem. Biophys.* **1975**, *169*, 344−353.
(28) Clark, W. M. *Oxidation−Reduction Potentials of Organic Systems*; William & Wilkins Co.: Baltimore, MD, 1960.
(29) Atkins, W. M.; Sligar, S. G. *J. Am. Chem. Soc.* **1987**, *109*, 3754−3760.
(30) Loida, P. J.; Sligar, S. G. *Biochemistry* **1993**, *32*, 11 530−11 538.

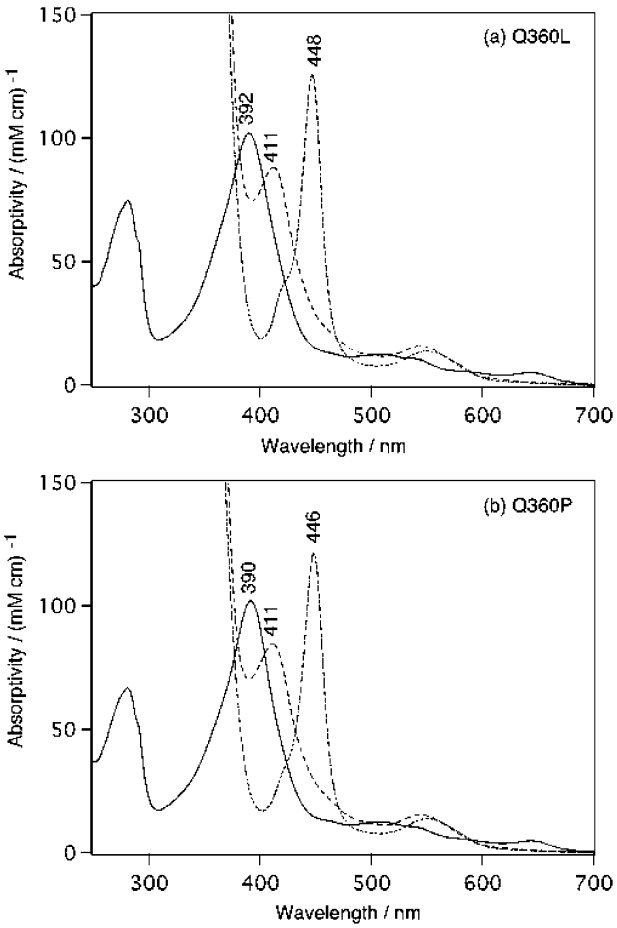

Figure 2. Optical absorption specta of the Q360L (panel a) and Q360P (panel b) mutants of $P450_{cam}$ in the presence of 1-mM *d*-camphor, 50-mM potassium phosphate at pH 7.4 and 100-mM KCl. The solid, broken, and dotted lines indicate the spectra for the ferric, ferrous, and ferrous-carbonmonoxy forms of the mutants, respectively.

added to 500 μL of the acidified aliquot of the reaction mixture, and the absorbance of the mixture was measured at 480 nm. The amount of H_2O_2 formed was calculated from a standard curve determined using a stock H_2O_2 solution.

Results

Electronic Absorption Spectroscopy. UV/vis spectra for the ferric, ferrous, and ferrous-CO forms of Q360L and Q360P were obtained to examine the coordination structure of the heme iron (Figure 2). The ferric Q360L exhibited the same spectrum as the ferric wild-type enzyme. Although the Soret maximum of the ferric Q360P showed a 2 nm blue shift, the overall spectral shapes and extinction coefficients were indistinguishable from those of the wild-type enzyme. The reduced form of the two mutants possessed the Soret maximum at 411 nm, which indicates the increased electron density on the thiolate in the reduced state.[14] The CO-bound ferrous form of Q360L and Q360P showed a Soret maximum at 448 and 446 nm, respectively, which supports the presence of the iron−sulfur coordination.[31] Furthermore, the red-shifted Soret maximum for the ferrous-CO form of Q360L suggests an increase of electron density on the thiolate.[14] As we reported previously, the Soret maxima for the ferric, ferrous, and ferrous-CO forms of L358P appear at 392, 409, and 445 nm, respectively.[22] These results indicate that Q360L and Q360P maintain the heme-thiolate

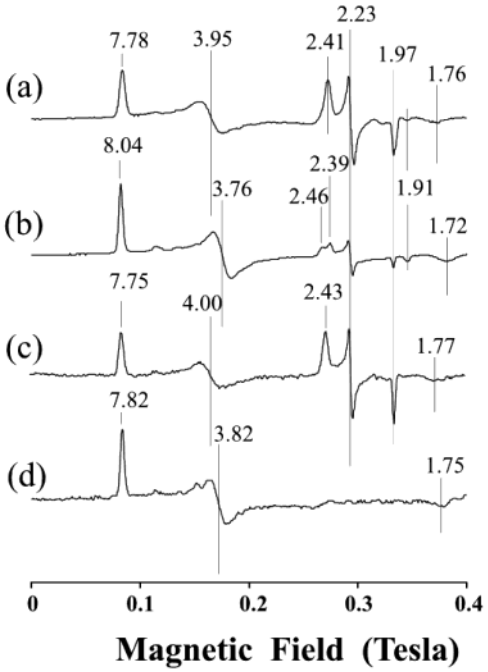

Figure 3. Electron paramagnetic resonance (EPR) spectra of the ferric form of the wild-type $P450_{cam}$ (trace a), L358P (trace b), Q360L (trace c) and Q360P (trace d) mutants observed at 15 K. The enzymes were dissolved in 50-mM potassium phosphate buffer at pH 7.4 containing 100-mM KCl and 1-mM *d*-camphor.

coordination. We should point out, however, that the removal of *d*-camphor in Q360P resulted in the conversion of the mutant to P420 as evidenced in a large fraction of 422 nm species in the ferrous-CO form (not shown). This observation implies that the amide proton at position 360 has a role in stabilizing the iron-thiolate bond.

Electron Paramagnetic Resonance (EPR) Spectroscopy. We measured EPR spectra of Q360L and Q360P to examine the coordination geometry of the ferric enzymes. Figure 3 illustrates the comparison of the EPR spectra for the Q360 mutants, wild type and L358P measured at 15 K. The wild-type $P450_{cam}$, in the presence of *d*-camphor, gave a mixture of rhombic high-spin species (g = 7.78, 3.95, and 1.76) and low-spin species (g = 2.41, 2.23, and 1.97).[32−34] The low-spin species is derived from the water-bound heme that appears only at the cryogenic temperature.[32−34] All ferric enzymes are in the high-spin state at room temperature as evidenced in the optical absorption spectra. The g-values of the low- and high-spin species of Q360L were almost the same as those of the wild type. In addition, the ratio of the amounts of the low- and high-spin species was almost the same as that of the wild type, indicating the similar iron-thiolate coordination geometries. On the other hand, the low-spin species disappeared completely in Q360P. The observation implies that the coordination of a water molecule trans to the heme is perturbed at 15 K in Q360P. Two weak signals from low-spin complexes were resolved in the spectrum of L358P at g_z = 2.46 and 2.39. Both components are different from that of the substrate-free low-spin species

(31) Gunsalus, I. C.; Wagner, G. C. *Methods Enzymol.* **1978**, *52*, 166−188.
(32) Tsai, R.; Yu, C.-A.; Gunsalus, I. C.; Peisach, J.; Blumberg, W. E.; Orme-Johnson, W. H.; Beinert, H. *Proc. Natl. Acad. Sci. U.S.A.* **1970**, *66*, 1157−1163.
(33) Lipscomb, J. D. *Biochemistry* **1980**, *19*, 3590−3599.
(34) Masuya, F.; Tsubaki, M.; Makino, R.; Hori, H. *J. Biochem.* **1994**, *116*, 1146−1152.

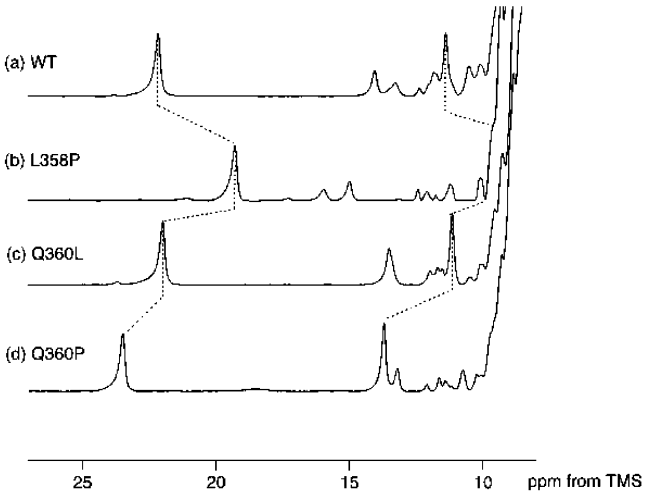

Figure 4. ^{1}H NMR spectra of the cyanide-adduct of the wild-type P450$_{cam}$ (trace a), L358P (trace b), Q360L (trace c) and Q360P (trace d) mutants. The spectra were obtained at 290 K in 50-mM potassium phosphate buffer at pH 7.4 containing 1-mM *d*-camphor, 100-mM KCl, 10% D_2O, and 10-mM KCN.

for L358P (g = 2.44, 2.25, and 1.91, not shown), and are probably due to the two different orientations of the thiolate ligand.

The *g*-values obtained for the high-spin component reflect the structural perturbation at the heme environment.[30,31] The observed *g*-values for both Q360P (g = 7.82, 3.82, and 1.75; rhombicity, 25%) and L358P (g = 8.04, 3.76, and 1.72; rhombicity, 26.8%) are more anisotropic than those in the wild type (g = 7.78, 3.95, and 1.76; rhombicity, 23.9%) and Q360L (g = 7.75, 4.00, and 1.77; rhombicity, 23.4%).[35] We suggest that the removal of the amide protons at 358 and 360 slightly modulates the geometry of the iron-thiolate bond, and causes a different amount of low-spin component at the low temperature.

Proton Nuclear Magnetic Resonance (^{1}H NMR) Spectroscopy. The structural perturbation to the iron-thiolate ligation by the mutations of residues at 358 and 360 were further confirmed by ^{1}H NMR spectra for the cyanide-bound (CN^-) ferric mutants. Figure 4 shows the paramagnetic ^{1}H NMR shifts of the heme substituents for the cyanide-bound form of the wild type, L358P, Q360L, and Q360P. The hyperfine shifted NMR peaks at 22.2 and 11.4 ppm for the wild-type P450$_{cam}$ have been assigned to 5- and 1-methyl groups of the heme, respectively.[36] Q360L resulted in almost the same spectrum as that of the wild-type enzyme (Figure 4c). Both methyl signals showed upfield shifts by ~3 ppm for L358P (Figure 4b), although they showed downfield shifts by 1~2 ppm for Q360P (Figure 4d). The opposite shifts of the heme methyl signals between L358P and Q360P indicate that the amide protons at positions 358 and 360 give opposite electronic and/or structural perturbations to the iron-thiolate bond.

Resonance Raman Spectroscopy. To examine the coordination structures and the electronic perturbations on the heme group in the Q360 mutants, we obtained resonance Raman spectra in the various oxidation and coordination states. The heme iron oxidation state marker (ν_4), the ligation state marker (ν_3), and two other Raman lines susceptible to the spin and coordination states (ν_2 and ν_{10}) were used to characterize the heme active site of the ferric and ferrous mutants (Supporting Information and Table 1).[37] It is well-known that the ν_4 line is sensitive to the π-electron density in the π^* antibonding orbitals of the porphyrin ring. Because we observed almost no change in the frequency of ν_4 line for both ferric and ferrous forms of the mutants, the electron density on the heme macrocycle was not significantly affected by the proximal mutations. The other marker lines (ν_3, ν_2, and ν_{10}) were also insensitive to the mutations. These results indicate that the current mutations do not modulate the coordination structure, spin state, and electronic structure of the heme macrocycle at room temperature.

Table 1. Frequencies of Resonance Raman Lines (cm^{-1}) in the High Frequency Region of the Ferric and Ferrous Forms of the Wild Type P450$_{cam}$, and the L358P, Q360L, and Q360P Mutants

	ν4	ν 3	ν 2	ν 10
ferric wild-type	1370	1487	1569	1622
ferric L358P	1371	1487	1569	1623
ferric Q360L	1370	1487	1569	1622
ferric Q360P	1369	1488	1570	1623
ferrous wild-type	1345	1467	1562	1600
ferrous L358P	1346	1467	1564	1601
ferrous Q360L	1344	1467	1563	1601
ferrous Q360P	1344	1468	1565	1600

Table 2. Frequencies of Resonance Raman Lines (cm^{-1}) for the Fe−XO (X = C and N) Stretching and the Fe-X−O Bending Modes in the Ferrous State and for the Fe−S Stretching Frequencies in the Ferric State Observed for the Wild Type P450$_{cam}$, and for the L358P, Q360L, and Q360P Mutants

	ν_{Fe-CO}	δ_{Fe-CO}	ν_{Fe-NO}	δ_{Fe-NO}	ν_{Fe-S}
wild type	484	561	552	446	351
L358P	489	559	553	447	351
Q360L	483	561	556	446	351
Q360P	482	559	557	448	347

We next examined the Fe−S stretching mode of the oxidized enzymes in the presence of *d*-camphor by the laser excitation at 363.8 nm (Supporting Information and Table 2). The Fe−S stretching mode appeared at 351 cm^{-1} for the wild-type enzyme, which is consistent with the previous results.[38,39] The Fe−S stretching modes for L358P and Q360L were also observed at 351 cm^{-1}, indicating no change in the strength of the Fe−S bond. On the other hand, Q360P showed a downshift by 4 cm^{-1}, indicating a perturbation on the Fe−S bond in the oxidized Q360P mutant.

We also obtained resonance Raman spectra for the reduced CO- and NO-bound forms of the enzymes (Figure 5 and Table 2). The trans axial ligands are known to affect the bond strengths of both Fe−XO and X−O (X = C and N).[40−45] However,

(35) Palmer, G. In *The Porphyrins*; Dolphin, D., Ed.; Academic Press: New York, 1979; Vol. IV, pp 313−353.
(36) Mouro, C.; Bondon, A.; Jung, C.; De Certaines, J. D.; Simonneaux, G. *Eur. J. Biochem.* **2000**, *267*, 216−221.
(37) Spiro, T. G.; Li, X,-Y. In *Biological Applications of Raman Spectroscopy*; Spiro, T. G., Ed.; Wiley-Interscience: New York, 1988; Vol. III; pp 1−38.
(38) Wells, A. V.; Li, P.; Champion, P. M.; Martinis, S. A.; Sligar, S. G. *Biochemistry* **1992**, *31*, 4384−4393.
(39) Unno, M.; Christian, J. F.; Benson, D. E.; Gerber, N. C.; Sligar, S. G.; Champion, P. M. *J. Am. Chem. Soc.* **1997**, *119*, 6614−6620.
(40) Unno, M.; Christian, J. F.; Sjodin, T.; Benson, D. E.; Macdonald, I. D. G.; Sligar, S. G.; Champion, P. M. *J. Biol. Chem.* **2002**, *277*, 2547−2553.
(41) Kerr, E. A.; Yu, N.-T. In *Biological Applications of Raman Spectroscopy*; Spiro, T. G., Ed.; Wiley-Interscience: New York, 1988, Vol. III; pp 39−95.
(42) Ray, G. B.; Li, X.-Y.; Ibers, J. A.; Sessler, J. L.; Spiro, T. G. *J. Am. Chem. Soc.* **1994**, *116*, 162−176.
(43) Spiro, T. G. In *Iron Porphyrins*, Part II; Lever, A. B. P., Gray, H. B., Ed.; Addison-Wiley: Reading, MA, 1983 pp 89−159.
(44) Li, X. Y.; Spiro, T. G. *J. Am. Chem. Soc.* **1988**, *110*, 6024−6033.
(45) Vogel, K. M.; Kozlowski, P. M.; Zgierski, M. Z.; Spiro, T. G. *J. Am. Chem. Soc.* **1999**, *121*, 9915−9921.

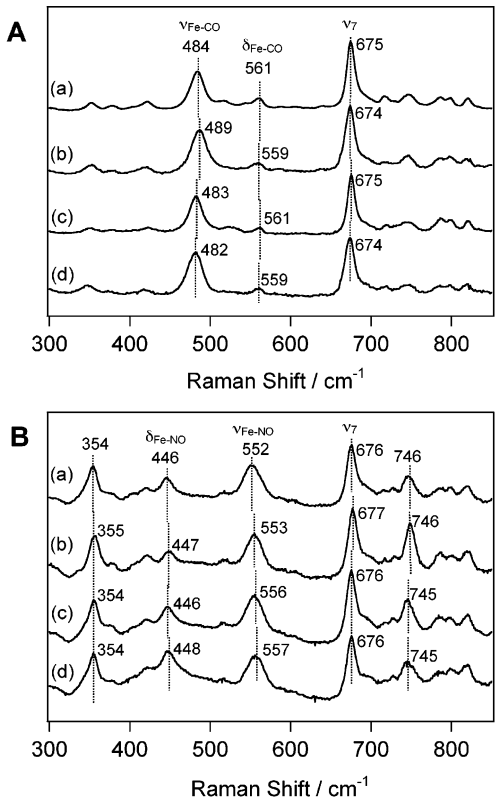

Figure 5. Resonance Raman spectra of the ferrous CO-bound form (panel A) and the ferrous NO-bound form (panel B) of the wild-type $P450_{cam}$ (trace a), L358P (trace b), Q360L (trace c) and Q360P (trace d) mutants excited at 441.6 nm. All sample solutions contained 15-μM $P450_{cam}$, 50-mM potassium phosphate buffer at pH 7.4, 100-mM KCl and 1-mM *d*-camphor.

although the Fe−CO and C═O frequencies (ν_{Fe-CO} and $\nu_{C=O}$) also depend on polarity of the heme distal side,[40−46] it is established that the Fe−NO stretching frequency (ν_{Fe-NO}) is rather insensitive to changes in the distal polarity.[40,45] Therefore, it is essential to obtain both spectra to clarify the structural and electronic perturbations on the Fe−S bond by the current mutations.

The Fe−CO stretching frequencies of the CO-bound Q360L and Q360P were observed at 483 and 482 cm^{-1}, respectively. The observed shifts were 1∼2 cm^{-1} toward lower frequency and were opposite direction from that of L358P (489 cm^{-1}).[22] We obtained a set of peaks at 446 and 552 cm^{-1} for the NO-bound reduced form of the wild-type enzyme, which were assigned to the Fe−NO bending and stretching modes, respectively.[40,47] Although L358P gave almost the same shifts as those of wild type, Q360L afforded upshift for the stretching frequency by ∼4 cm^{-1} without changing the bending frequency. The ∼2 and ∼5 cm^{-1} of upshifts in the bending and stretching frequencies, respectively, were found for Q360P. To summarize, we found different electronic perturbations on the Fe-ligand bonds in the reduced enzymes as a result of removals of the amide protons at positions 358 and 360.

Catalytic Activity of the Q360 Mutants. To examine the catalytic activity of the constructed mutants, we measured the NADH consumption rates for the *d*-camphor oxidation with changing the amount of Pdx, and obtained K_m and V_{max} values using Michaelis−Menten analysis (Table 3). The first electron transfer (ET) between Pdx and $P450_{cam}$ is the rate-limiting reaction in the current condition of the activity measurement. The V_{max} values of 62%, 49%, and 75% compared to V_{max} for the wild-type enzyme were found for L358P, Q360P, and Q360L, respectively. L358P had ∼2-fold increased affinity (K_m) for Pdx, although the Q360 mutants showed almost the same affinities as that of the wild-type enzyme. We further measured the redox potentials of the mutants (Table 3). The redox potentials of Q360L and Q360P were −180 ± 5 mV and −205 ± 5 mV, respectively, which are significantly lower than those of wild type (−134 ± 3 mV) and L358P (−170 ± 2 mV).[22] The lowered redox potentials of the Q360 mutants are consistent with their reduced V_{max} values.

Table 3. Michaelis−Menten Parameters (K_m and V_{max}) for the Electron Transfer Reaction from Pdx to the Wild Type $P450_{cam}$, L358P, Q360L, and Q360P Mutants[a]

	K_m (μM)	V_{max} (μM/min)	redox potential (mV)
wild type	10.6	1115	−134 ± 3
L358P	5.2	688	−170 ± 2
Q360L	9.5	835	−180 ± 5
Q360P	12.6	550	−205 ± 5

[a] The reduction potentials for the Fe(III)/Fe(II) Couple of the $P450_{cam}$ samples were also indicated. The K_m and V_{max} parameters were obtained from the steady-state measurements of the overall *d*-camphor oxidation at the various concentration of Pdx.

To confirm that the alterations of the ET rates can be explained from the redox potential changes of the mutants, we calculated the ET rates based on the Marcus equation given as follows[48]

$$k_{ET} = \frac{4\pi^2 H_{AB}{}^2}{h(4\pi\lambda RT)^{1/2}} \exp\left[-\frac{(\Delta G + \lambda)^2}{4\lambda RT}\right]$$

where k_{ET} is the ET rate, h is Plank's constant, R is the gas constant, T is temperature, λ is the reorganization energy, $\Delta G°$ is the redox potential difference between donor and acceptor, and H_{AB} is the degree of wave function overlap between donor and acceptor. We assumed that all parameters except for $\Delta G°$ are not perturbed by the mutations and that the redox potential of Pdx is −215 mV.[25] Furthermore, the λ values from 0.4 to 1.2 eV were tentatively used. The calculated k_{ET} values based on the measured redox potentials of the mutants are 52∼55, 27∼29, and 43∼46% of that of the wild-type enzyme for L358P, Q360P, and Q360L, respectively. Considering the approximate nature of the calculations, these values are comparable to the observed reductions of the V_{max} values (62, 49, and 75% for L358P, Q360P, and Q360L, respectively), and indicate that the reduced ET rate can be explained by the changes of the reduction potentials of the mutants.

To examine the O−O bond cleavage step, we next employed cycloohexane and styrene as substrates in the reconstituted system containing NADH, PdR, and Pdx.[22] The unnatural substrates often give uncoupling products such as O_2^- and H_2O_2, whose yields reflect the efficiencies of the elementary steps in the P450 catalysis.[49−51] Thus, determination of the yields of the oxidized products and H_2O_2 is important to monitor the efficiency of the O−O bond scission step.[51] Table 4 presents

(46) Spiro, T. G.; Zgierski, M. Z.; Kozlowski, P. M. *Coord. Chem. Rev.* **2001**, 219−221, 923−936.
(47) Hu, S.; Kincaid, J. R. *Biochemistry* **1991**, *113*, 9760−9766.
(48) Marcus, R. A.; Sutin, N. *Biochim. Biophys. Acta* **1985**, *811*, 265−322.

Table 4. NADH Turnover, Total Product Formation Rates and Coupling Efficiencies of Hydrocarbon Oxidation Catalyzed by the Wild Type P450$_{cam}$, L358P, Q360L, and Q360P Mutants

substrate	product	enzyme	NADH turnover[a]	product rate[b] (% coupling)[c]	uncoupling (%)[d]
		wild type	21.6	3.6 (8.3)	59.8
styrene	styrene oxide	L358P	26.4	14.2 (26.9)	40.9
		Q360L	24.6	4.2 (12.3)	49.4
		Q360P	17.6	3.1 (12.5)	49.5
		wild type	53.6	32.4 (30.3)	40.9
cyclohexane	cyclohexanol	L358P	60.4	58.9 (48.8)	22.0
		Q360L	57.6	17.1 (29.7)	48.7
		Q360P	33.7	19.6 (29.1)	46.9

[a] μM/min. [b] μM/μM P450$_{cam}$/min. [c] The coupling is the ratio of the total amount of products formed to the total amount of NADH consumed and expressed as a percentage. [d] The uncoupling is the ratio of the amount of hydrogen peroxide formed to the amount of NADH consumed.

the NADH consumption rates, product formation rates, coupling and uncoupling efficiencies in the reaction with styrene and cyclohexane. It is clearly shown that the product formation rates of L358P for styrene and cyclohexane were 3.9 and 1.8 times faster than those of the other enzymes, respectively. More importantly, Q360L and Q360P did not show any significant changes in the yields of the product formations (coupling) and the H_2O_2 production (uncoupling) compared with those of the wild-type enzyme within our experimental errors. In contrast, L358P enhanced the coupling and depressed the uncoupling, which correspond to the promotion of the O−O bond scission.[22] The small effects observed in the activities of the Q360 mutants imply that the increased electronegativity of the thiolate ligand does not always promote the O−O bond heterolysis.

Discussion

Structural Roles of the Amide Proton at Position 360. The amide protons of P450$_{cam}$ were removed by the single mutations of the proximal residues at positions 358 and 360 with proline. We successfully purified Q360P in the presence of *d*-camphor, although its yield was ca. 1/20 of that for the wild-type enzyme (data not shown). Q360P is also stable in various coordination and oxidation states as long as *d*-camphor is present, but easily converts to P420 when *d*-camphor is removed. In contrast, Q360L having the NH−S hydrogen bond at position 360 did not convert to P420 in the absence of *d*-camphor. Therefore, we conclude that the amide proton at position 360 in P450$_{cam}$ is critical to stabilize the coordination of the thiolate ligand to the heme iron especially in the absence of *d*-camphor. Our previous study indicated that the amide proton-deficient L358P does not cause a significant instability of the enzyme even in the absence of *d*-camphor.[22] Because a proline residue is naturally observed at the residue adjacent to the thiolate ligand in CPO and plant P450s,[1,10] the amide proton at position 358 is not essential for the structural maintenance of the heme-thiolate enzymes. Furthermore, the stability of Q360L indicates no essential role of the hydrogen bond between the side chain amide of Gln360 and the carbonyl oxygen of Cys357 for the maintenance of the cysteine coordination in P450$_{cam}$.

In contrast to the apparent reduction in the stability of the enzyme, the current mutations did not induce a large structural alteration on the heme coordination and environmental structures. First, we observed no changes in the spin state of the heme at room temperature as evidenced in the optical absorption and resonance Raman spectroscopies. Second, the K_m values obtained by the Michaelis−Menten analysis are within a factor of 2 of that obtained for the wild-type enzyme. The V_{max} values are also consistent with the calculated ET rates that assume only the changes in the redox potentials. Because the position 360 is likely involved in the interface between P450$_{cam}$ and Pdx,[52] we can consider that the changes caused by the mutations are rather small. We conclude that the P450$_{cam}$ mutants constructed in this study maintain the heme proximal structures that are required for the electron transfer and the activity of P450$_{cam}$.

We would like to discuss briefly on the roles of the NH−S hydrogen bonding in relation to the strength of the Fe−S bond. The arene-thiolate compounds revealed that the formation of the NH−S hydrogen bond lengthens the Fe−S distance by ∼0.03 Å.[12,13] In contrast, the alkane-thiolate compound indicated that the Fe−S distance is shortened (∼0.02 Å) by the formation of the NH−S hydrogen bond.[14] The observed low-frequency shift of ∼5 cm^{-1} for the Fe−S stretching mode in Q360P is consistent with the alkane-thiolate study in direction; however, the shift is observed only for Q360P and is much smaller than the shift of ν_{Fe-S} reported for the alkanethiolate model (∼30 cm^{-1}). We suggest that these model compounds possess the stronger NH−S hydrogen bonds than the actual proteins. Furthermore, the above comparison indicates that the changes in the Fe−S bond length caused by the Q360P mutation should be smaller than 0.02 Å, and confirms that the structural alteration at the heme proximal site of the mutant is small.

Regulation of Reduction Potential of Heme by the Proximal Structure. It has been proposed that the NH−S hydrogen bonds regulate the redox potential of the heme-thiolate complexes.[12−15] We previously reported the −134 and −170 mV of the reduction potentials for wild type and L358P, respectively.[22] The present study further determined that the reduction potentials for Q360P and Q360L are −205 and −180 mV, respectively. To explain these observations, we propose the following relationship between the redox potentials and the numbers of the hydrogen bonds. We assume ca. −45 mV and −35 mV of changes in the redox potentials for the loss of a hydrogen bond between the carbonyl oxygen of Cys357 and the side chain amide of Gln360 and between the amide protons of polypeptide and the thiolate sulfur of Cys357, respectively. Because Q360L lacks the side chain of Gln, it indicates the negative shift by 45 mV (−180 mV). L358P lacks one of the amide protons, which lowers the redox potential by ∼35 mV (−170 mV). The observed value for Q360P is consistent with the summation of these two effects that is almost equivalent to ca. −70 mV (−205 mV). Thus, the proximal hydrogen bonding network including the NH−S and side chain hydrogen bonds regulates the reduction potential of the heme for P450$_{cam}$.

It is important to compare the current observations with the previous model complexes that possess the NH−S hydrogen bonds. Ueno et al. showed that the tetrapeptide-heme complex that mimicked the proximal structure of P450$_{cam}$ indicates

(49) Mueller, E. J.; Loida, P.; Sligar, S. G. In *Cytochrome P450 Structure, Mechanism, and Biochemistry*, 2nd ed.; Ortiz de Montellano, P. R., Ed.; Plenum Press: New York, 1995, pp 83−124.
(50) Nickerson, D. P.; Harford-Cross, C. F.; Fulcher, S. R.; Wong, L.-L. *FEBS Lett.* **1997**, *405*, 153−156.
(51) Kadkhodayan, S.; Coulter, E. D.; Maryniak, D. M.; Bryso, T. A.; Dawson, J. H. *J. Biol. Chem.* **1995**, *270*, 28 042−28 048.
(52) Tosha, T.; Yoshioka, S.; Hori, H.; Takahashi, S.; Ishimori, K.; Morishima, I. *Biochemistry*, in press.

30∼40 mV of negative shifts in the reduction potential by the formation of one NH−S hydrogen bond.[15] In contrast, large negative shifts of 100∼200 mV were observed in the model compound studies by Ueyama et al.[12,13] and by Suzuki et al.[14] The current results indicating ∼35 mV of the negative shift by the removal of an amide proton agree with that of the tetrapeptide work by Ueno et al.[15] The smaller shifts observed in the protein and peptide systems suggest that the individual hydrogen bonding between the cysteine sulfur and the surrounding amide protons are weak. In fact, the distances between the amide proton and the sulfur atom in the model system reported by Ueyama et al. (∼2.4 Å) are shorter than the distances estimated for the protons at 358 (3.34 Å) and 360 (2.82 Å) (Figure 1).

It should be stressed that the removal of a single hydrogen bond from the heme proximal site induces the significant changes in the redox potential of $P450_{cam}$. The susceptibility of the enzymatic function to the proximal structure is consistent with the recent agreement that the reactivity of $P450_{cam}$ are regulated by the complex formation with Pdx that associates with $P450_{cam}$ at the proximal site. It has been reported that the complex formation is accompanied by electronic and structural changes around the axial thiolate ligand of $P450_{cam}$.[39,40,52,53] We propose that the electronic and structural perturbations on the thiolate ligand modulated by the proximal hydrogen bond network are critical for the functions of $P450_{cam}$, especially in the regulation of the redox potential of the heme.

Increase of σ-Electron Donation by the Mutations at Position 360. The present results of resonance Raman spectroscopy can be explained by considering the increase in the σ- and π-electron donations of the axial thiolate to the Fe−CO and Fe−NO moieties. Because the iron atom back-donates π-electron to the CO π^* orbital, the observed up- and downshifts of ν_{Fe-CO} and ν_{C-O}, respectively, in L358P can be explained by the increased π-electron donation from the thiolate ligand through the iron orbital.[41−46] On the other hand, ν_{Fe-CO} of the Q360 mutants indicated the opposite low-frequency shifts, suggesting the stronger σ-bonding of the thiolate ligand that weakens the trans Fe−CO bond.[41−46] In contrast to ν_{Fe-CO}, ν_{Fe-NO} is known to indicate upshifts upon the increase in the σ-electron donation from the trans axial ligand.[40,45] Thus, the increase in the Fe−NO stretching frequencies by 4∼5 cm^{-1} also supports the increased σ-electron donation of the thiolate in the Q360 mutants.[40,45] The consistent explanation for the shifts in the Fe−CO and Fe−NO stretching frequencies by the same proximal effects supports small structural alteration in the heme distal sites of the mutants. We note that the stronger σ-electron donation of the Q360 mutants is not only due to the disruption of the amide proton, because Q360L showed the same shifts in the Fe−XO (X = C and N) and C−O stretching frequencies.

The difference in the electronic effects by the L358P and Q360P mutants is consistent with the NMR results. Although the proton hyperfine shifts in ^1H NMR spectra for cyanide-bound $P450_{cam}$ have not been fully investigated, we can infer the origins of the shifts by referencing to the cyanide-bound metmyoglobin. The hyperfine shifts of the methyl protons in cyanomet-myoglobin correlate with the overlap of the iron d_{xz} and d_{yz} orbitals with the p_π orbital of the axial imidazole.[54] Since the unpaired electron possesses more density along the N_1-N_3 vector due to the overlap with the p_π orbital of the imidazole, the hyperfine shifts for 5- and 1-methyl groups are observed in cyanomet-myoglobin. The hyperfine shifts observed in cyanide-bound $P450_{cam}$ could also be explained by the overlap of the p_π-orbitals on the sulfur atom and the d-orbitals of the iron. The assignments of 5- and 1-methyl groups in $P450_{cam}$[36] suggest that the lone pairs of the thiolate expand along the porphyrin N_1-N_3 vector. The observed opposite shifts of the methyl resonances in Q360P and L358P suggests different electronic perturbations from the thiolate to the heme iron induced by the loss of the amide protons at position 358 and 360.

The increased σ-electron donation of the Q360 mutants can be rationalized by the location of the amide protons in the crystal structures of $P450_{cam}$ as shown in Figure 1. Interestingly, the proton at 360 is located very close to the normal of heme plane. In contrast, the proton at 358 approaches the thiolate sulfur almost from the equatorial position. It is reasonable to conclude that the proton at 360 mainly modulates the σ-electron, whereas the proton at 358 mainly modulates the π-electron of the thiolate ligand.

Roles of the Push Effects in the Heterolysis of Dioxygen. If the electronic push effect from the axial thiolate facilitates the O−O bond heterolysis in $P450_{cam}$, as has been hypothesized in the common "push−pull" mechanism,[55−58] all the three mutants should enhance heterolysis. However, although L358P promoted the heterolysis of dioxygen, both of the Q360 mutants did not show appreciable changes in the O−O bond scission of dioxygen compared with the wild-type enzyme. Similarly, a recent model compound study by Nam et al. argues against the classical "push−pull" mechanism,[59] although many model studies demonstrated that the O−O bond heterolysis of acyl-peroxo-iron (III) porphyrin complexes is accelerated by the push effect of axial ligands.[3,55−58] Furthermore, Roach et al. investigated the peroxidase activities of myoglobin mutant (H93G) with substituted imidazoles as proximal ligands,[60,61] and found that the rates of the O−O bond scission increase only 1.7-fold for each increase of 1 pK_a unit of the axial imidazoles. It might be necessary to reinterpret the electronic push effects of the axial ligand for the O−O bond heterolysis.

One possibility that might explain the current observation is that the rate determining step of the O−O bond activation is different between L358P and Q360P. However, the explanation is less likely, because both mutations similarly remove one of the NH−S hydrogen bonds, whose effects on the O−O bond activation pathway should not be drastically different. Instead, we propose that the driving force for the O−O bond heterolysis is the π-push effect of the axial thiolate. The critical step in the

(53) Sjodin, T.; Christian, J. F.; Macdonald, I. D. G.; Davydov, R.; Unno, M.; Sligar, S. G.; Hoffman, B. M.; Champion, P. M. *Biochemistry* **2001**, *40*, 6852−6859.
(54) Yamamoto, Y.; Nanai, N.; Chujo, R.; Suzuki, T. *FEBS Lett*. **1990**, *264*, 113−116.
(55) Poulos, T. L.; Kraut, J. *J. Biol. Chem*. **1980**, *255*, 8199−8205.
(56) Groves, J. T.; Han, Y.-Z. In *Cytochrome P450 Structure, Mechanism, and Biochemistry*, 2nd ed; Ortiz de Montellano, P. R., Ed.; P. R. Plenum Press: New York, 1995, pp 3−48.
(57) Watanabe, Y. In *Oxygenase and Model Systems*; Funabiki, T., Ed.; Kluwer Acadenic Publisher: The Netherlands, 1997, pp 223−282.
(58) Watanabe, Y. In *The Porphyrin Handbook*, Vol. 4; Kadish, K. M., Smith, K. M., Guilard, R., Ed.; Academic Press: New York, 2000, pp 97−117.
(59) Nam, W.; Han, H. J.; Oh, S.-Y.; Lee, Y. J.; Choi, M.-H.; Han, S.-Y.; Kim, C.; Woo, S. K.; Shin, W. *J. Am. Chem. Soc*. **2000**, *122*, 8677−8684.
(60) Roach, M. P.; Ozaki, S.; Watanabe, Y. *Biochemistry* **2000**, *39*, 1446−1454.
(61) Ozaki, S.; Roach, M. P.; Matsui, T.; Watanabe, Y. *Acc. Chem. Res*. **2001**, *34*, 818−825.

O−O bond heterolysis is considered to be the protonation of the hydroperoxide ligand in compound 0. As suggested previously, the protonation to the outer oxygen atom in compound 0 will lead to the facile heterolysis of the O−O bond.[62] The increased π-electron density of the thiolate increases the double bond character of the trans Fe−O bond, and in turn promotes the protonation of the outer oxygen atom as indicated in the following resonance structures.

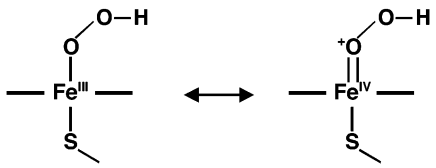

In contrast, the strong σ-electron donation from the axial thiolate to the iron d_{z^2} should favor the release of the trans $^{-}$OOH ligand of compound 0 by an electronic repulsion rather than the O−O bond heterolysis, the phenomenon commonly known as the trans effect.[63] The present observations can be interpreted that the increase of the "π-push" effect of the axial ligand facilitates the heterolysis of the O−O bond in compound 0.

In summary, we have thoroughly investigated roles of the proximal hydrogen bonding network on P450$_{cam}$ functions by removals of the amide protons at the proximal cysteine ligand loop. We found that the proximal structure regulates the stability of the protein and the coordination geometry of the Fe−S bond, as well as the redox potential of the heme iron. Furthermore, we observed two kinds of electronic contributions from the thiolate ligand, that is, σ- and π-push effects, and proposed that the enhanced heterolysis by the increased π-electron donation of the thiolate ligand may account for the roles of the push effect in the O−O bond scission of dioxygen. We could not obtain information on the electronic structures of compound I for the NH−S hydrogen bond deficient mutants. Further investigations are necessary to confirm the predictions made by Shaik et al.[16,17] We are currently conducting the X-ray structural analysis of L358P to clarify the roles of the cysteine ligand loop in the catalytic cycle of P450$_{cam}$.

Note. After the submission of this work, Ogliaro et al. reported that σ-donor capability of the thiolate ligand is crucial for its push effect based on density functional calculation (Ogliaro, F., de Visser, S. P., Shaik, S. *J. Inorg. Biochem.* **2002**, *91*, 554−567). They also found that the π-donor capability of the thiolate does not affect the stability of compound I relative to the ferric hydroperoxide species. We point out that Ogliaro et al. did not evaluate the transition energies of the oxygen activation reactions.

Acknowledgment. We are indebted to Prof. Teizo Kitagawa (IMS, Okazaki) for his kind permission to use his resonance Raman instruments. We wish to acknowledge the reviewers for valuable suggestions in regard to the activities and the resonance Raman measurements for the Fe−S and Fe−NO stretching modes. This work was supported in part by grants-in-aid for scientific research on priority areas "Molecular Biometalics" (08249102 to I. M.) from the Ministry of Education, Science, Culture and Sports.

Supporting Information Available: Resonance Raman spectra for the Fe−S stretching mode of the wild type and the mutants of P450$_{cam}$, and resonance Raman spectra for the maker lines of the ferric and ferrous forms of the wild type and the mutants of P450$_{cam}$ (PDF). This material is available free of charge via the Internet at http://pubs.acs.org.

JA0265409

(62) Harris, D. L.; Loew, G. H. *J. Am. Chem. Soc.* **1998**, *120*, 8941−8948.
(63) Collman, J. P.; Hegedus, L. S.; Norton, J. R.; Finke, R. G. *Principles and Applications of Organotransition Metal Chemistry*; University Science Books: USA, 1987.